

Alfvén continuum and high-frequency eigenmodes in optimized stellarators

Ya. I. Kolesnichenko*, V. V. Lutsenko*, H. Wobig**,

Yu. V. Yakovenko*, and O. P. Fesenyuk*

**Scientific Centre “Institute for Nuclear Research”,*

03680 Kyiv, Ukraine

***Max-Planck Institut für Plasmaphysik, IPP-EURATOM*

Association, D-85748 Garching bei München, Germany

Outline

- Brief overview of previous results
- Basic equations
- Structure of Alfvén continuum in a Helias
- Discrete Alfvén eigenmodes
- Conclusions

AE in stellarators

Instabilities of tokamak-type AE (TAE, GAE) have been observed
[A. Weller et al., Phys. Rev. Lett. (1994)]

However, AE in stellarators may possess specific features

- The toroidal symmetry is broken
 - interaction of modes with different n is possible
- Rich spectrum of Fourier harmonics of B and g^{ij}
 - many possible continuum gaps
- Strong elongation (Helias)
- Small shear (Helias)

Helicity-induced continuum gaps and eigenmodes in a heliotron
[Nakajima, Cheng, Okamoto, Phys. Fluids B (1992)].

Numerical studies of Helias configurations with CAS3D
[Nührenberg, Phys. Plasmas (1999)].

- Helicity-induced gaps and discrete eigenmodes
- Effects of the ion sound

Present work

- Models as simple as reasonably possible
 \Rightarrow to proceed analytically as far as possible
- Analytical approximation of the metric tensor
- Gap modes
- Focus on the high-frequency part of the spectrum
 \Rightarrow effects of the ion sound are neglected

Publications

- Report IPP III/261 (May 2000)
- 27th EPS Conference on Controlled Fusion and Plasma Physics (Budapest, June 2000)
- submitted to Phys. Plasmas

Basic equations

To derive reduced linear MHD equations, we use one-fluid MHD and make the following assumptions:

- $\tilde{B}_\parallel = 0$ (incompressibility)
 $\rightarrow \vec{\tilde{A}}_\perp = 0$
- $\tilde{E}_\parallel = 0$ (ideal approximation)
- Effects of the plasma pressure are disregarded
- Equilibrium current is neglected (optimized stellarators)

We obtain:

$$\hat{L} \frac{\partial}{\partial x^i} \left[g_{\perp}^{ij} \frac{\partial}{\partial x^j} (\hat{L}\Phi) \right] + \omega^2 R_0^2 \frac{\partial}{\partial x^i} \left(\frac{g_{\perp}^{ij}}{\bar{v}_A^2 h^4} \frac{\partial \Phi}{\partial x^j} \right) = 0,$$

where Φ is the scalar potential of the perturbation, $x^j = \psi, \theta, \phi$ are the Boozer coordinates, $g_{\perp}^{ij} = g^{ij} - b^i b^j$, $\vec{b} = \vec{B}_0/B_0$, subscripts “0” refer to equilibrium quantities, $\hat{L} = \partial/\partial\phi + \iota\partial/\partial\theta$, $R_0 = L/2\pi$ is the major radius, \bar{v}_A is the flux-surface-averaged Alfvén velocity, h characterizes the variation of B .

We need the metric tensor, with $g^{\psi\psi}$ being of special importance (it enters the highest-derivative terms).

The Helias reactor configuration studied here

- 5 field periods
- Strong toroidally modulated ellipticity (elongation) of the plasma cross section:
 $1.5 \leq \kappa(\phi) \leq 3.6$.

The main axis of the ellipse rotates, making half turn over one field period

- Linked-mirror magnetic field:

$$B = \bar{B}h,$$

$$h = 1 + \epsilon_B^{(00)} + \epsilon_B^{(10)} \cos(N\phi) + \epsilon_B^{(11)} \cos(\theta - N\phi) + \epsilon_B^{(01)} \cos(\theta),$$

with the mirror harmonic dominating,

$$\epsilon_B^{(10)} \approx 0.1 > \epsilon_B^{(11)} \gg \epsilon_B^{(01)}$$

- Almost vanishing toroidal current

- Weak shear:

$$0.87 \leq \iota \leq 0.99 \text{ for } \beta = 0;$$

$$0.82 \leq \iota \leq 0.93 \text{ for } \beta = 5\%$$

E. Strumberger et al., Report IPP III/249 (1999).

Metrics

We employ the near-axis expansion of the equilibrium [Garren, Boozer, Phys. Fluids B (1991)]

→ In the lowest order, flux surfaces are concentric ellipses.

We obtain:

$$g^{\psi\psi} = 2B_{(0)}(\phi)\{\delta(\phi) + \lambda(\phi)\cos[2\theta - 2\theta_0(\phi)]\}\psi,$$

where $B_{(0)}$ is the magnetic field at the axis, $\delta = [\kappa(\phi) + \kappa^{-1}(\phi)]/2$, $\lambda = [\kappa(\phi) - \kappa^{-1}(\phi)]/2$, κ is the elongation of the flux surfaces.

Assuming that,

$$B_{(0)} = \hat{B}[1 + \epsilon_B^{01}\cos(N\phi)], \quad \theta_0 = N\phi/2,$$

$$\delta = \delta_0 + \delta_1\cos(N\phi), \quad \lambda = \lambda_0 + \lambda_1\cos(N\phi),$$

we find:

$$g^{\psi\psi} := 2\psi\hat{B}\delta_0[1 + \epsilon_g^{01}\cos(N\phi) + \epsilon_g^{21}\cos(2\theta - N\phi) + \epsilon_g^{20}\cos(2\theta) + \epsilon_g^{01}\cos(2\theta - 2N\phi)],$$

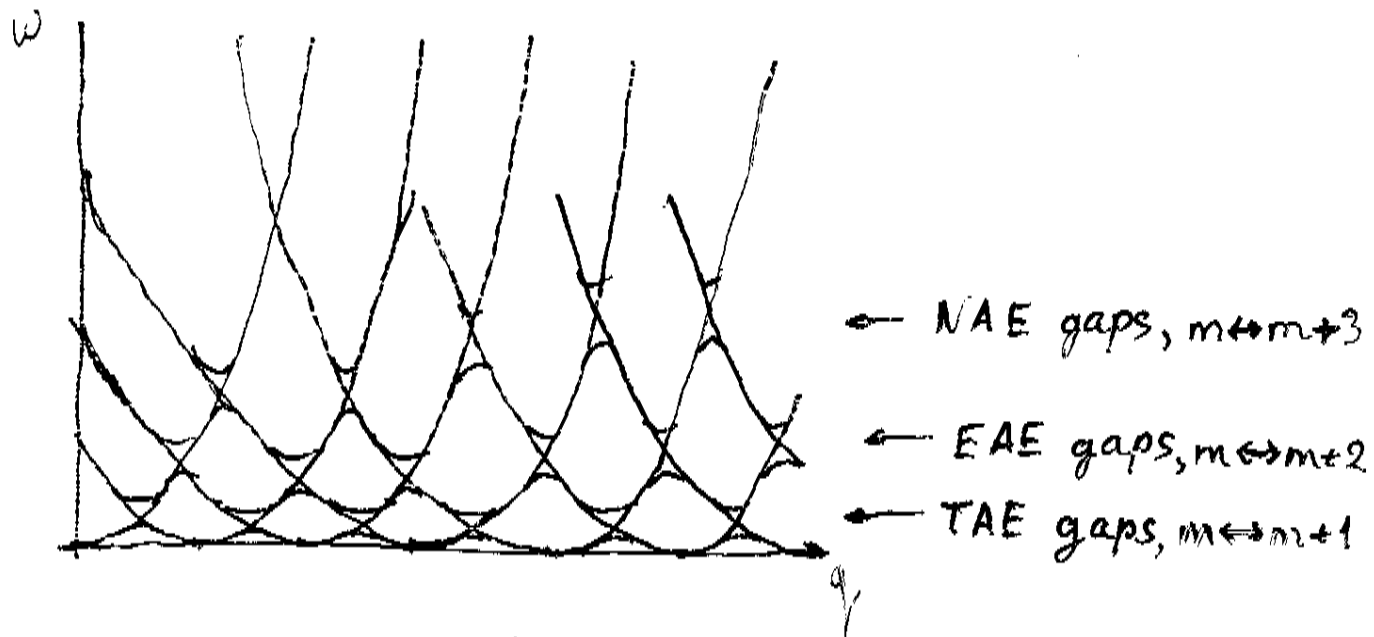
Equilibrium from [Strumberger et al., Report IPP III/249 (1999)]:

$$\kappa_{min} = 1.5, \kappa_{max} = 3.6, \epsilon_B^{01} = 0.1$$

$$\rightarrow \epsilon_g^{01} = 0.38, \epsilon_g^{21} = 0.68, \epsilon_g^{22} = \epsilon_g^{20} = 0.2.$$

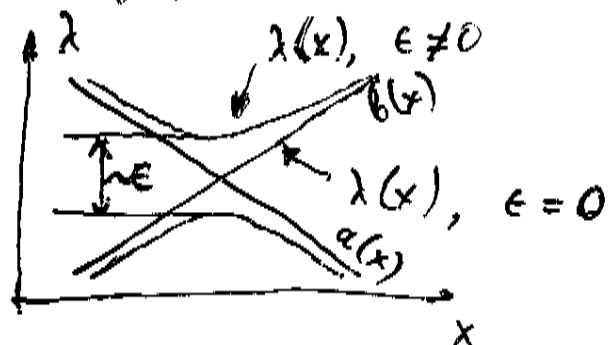
Alfvén eigenmodes (AE) in tokamaks

Alfvén continuum



Origin of the gaps

$$\begin{pmatrix} a(x) & \epsilon \\ \epsilon & b(x) \end{pmatrix}$$



Discrete Alfvén modes reside in the gaps and may be destabilized by high-energy ions

Structure of the Alfvén continuum

ω belongs to continuum when there is a flux surface ψ at which ω is an eigenvalue of the equation of local Alfvén resonance

$$\hat{L}(g^{\psi\psi}\hat{L}\Phi) + \omega^2 R_0^2 \frac{g^{\psi\psi}}{\bar{v}_A^2 h^4} \Phi = 0$$

The code COBRA (COntinuum BRanches of Alfvén waves): we take (for given m and n)

$$\Phi = \sum_{\mu,\nu=-\infty}^{\infty} \Phi_{\mu\nu} \exp[i(m+\mu)\theta - i(n+\nu N)\phi].$$

$$g^{\psi\psi} = g_0 \left[1 + \frac{1}{2} \sum_{\mu,\nu=-\infty}^{\infty} \epsilon_g^{(\mu\nu)} \exp(i\mu\theta - i\nu N\phi) \right],$$

$$g^{\psi\psi} h^{-4} = g_0 \left[1 + \frac{1}{2} \sum_{\mu,\nu=-\infty}^{\infty} \epsilon_c^{(\mu\nu)} \exp(i\mu\theta - i\nu N\phi) \right],$$

and obtain the eigenvalue problem for infinite matrices:

$$\sum_{\mu,\nu=-\infty}^{\infty} \mathcal{G}_{\mu*,\nu*;\mu,\nu} \Phi_{\mu\nu} = \omega^2 \frac{R_0^2}{\bar{v}_A^2} \sum_{\mu,\nu=-\infty}^{\infty} \mathcal{C}_{\mu*,\nu*;\mu,\nu} \Phi_{\mu\nu},$$

$$\mathcal{G}_{\mu*,\nu*;\mu,\nu} = \left(\delta_{\mu*\mu} \delta_{\nu*\nu} + \frac{1}{2} \epsilon_g^{(\mu*-\mu,\nu*-\nu)} \right) \tilde{k}_{\mu*\nu*} \tilde{k}_{\mu\nu},$$

$$\mathcal{C}_{\mu*,\nu*;\mu,\nu} = \delta_{\mu*\mu} \delta_{\nu*\nu} + \frac{1}{2} \epsilon_c^{(\mu*-\mu,\nu*-\nu)}$$

where $\tilde{k}_{\mu\nu} = \tilde{k} + \mu\iota - \nu N$, $\tilde{k} = m\iota - n$.

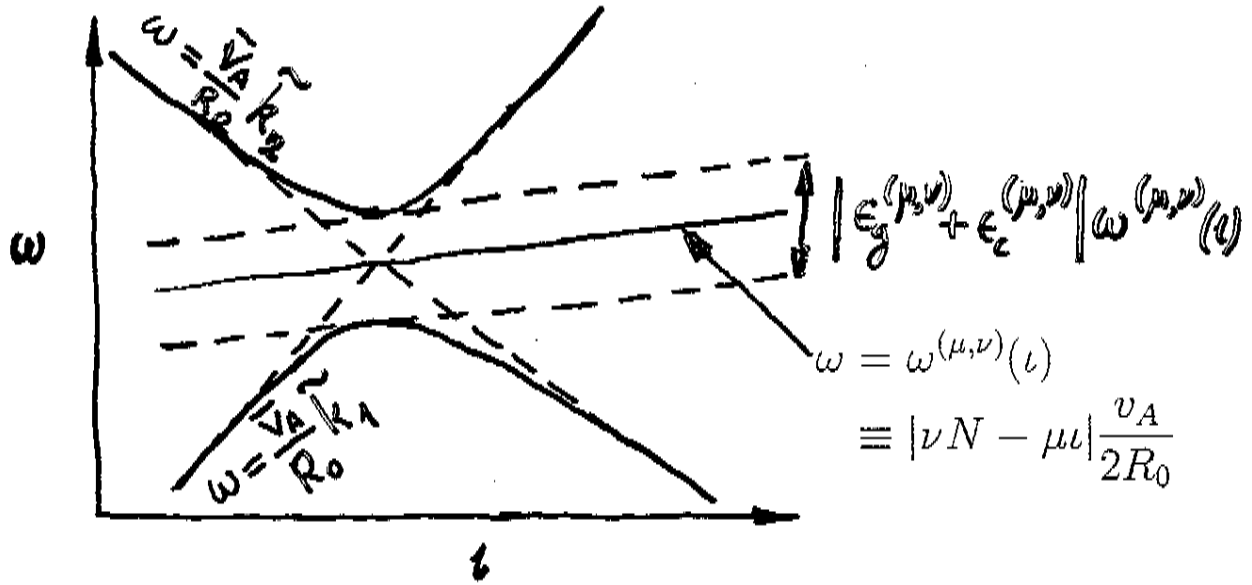
m and n do not appear explicitly anymore, only \tilde{k}_{\parallel} !

“Absolute” gaps

Let us assume that the mode coupling is weak and consider the interaction of only two modes, (m_1, n_1) and $(m_2 = m_1 + \mu, n_2 = n_1 + \nu N)$:

$$\begin{pmatrix} \tilde{k}_1^2 & \frac{1}{2}\epsilon_g^{(\mu,\nu)}\tilde{k}_1\tilde{k}_2 \\ \frac{1}{2}\epsilon_g^{(\mu,\nu)}\tilde{k}_1\tilde{k}_2 & \tilde{k}_2^2 \end{pmatrix} \begin{pmatrix} \Phi_1 \\ \Phi_2 \end{pmatrix} = \omega^2 \frac{r_0^2}{\bar{v}_A^2} \begin{pmatrix} 1 & \frac{1}{2}\epsilon_c^{(\mu,\nu)} \\ \frac{1}{2}\epsilon_c^{(\mu,\nu)} & 1 \end{pmatrix} \begin{pmatrix} \Phi_1 \\ \Phi_2 \end{pmatrix}$$

where $\tilde{k}_i(\iota) = m_i\iota - n_iN$.



- The branches with $m_2 - m_1 = \mu, n_2 - n_1 = \nu N$ meet (i.e., $\tilde{k}_1 = -\tilde{k}_2$) always at the line $\omega = \omega^{(\mu,\nu)}(\iota)$.
- The gap $|\omega - \omega^{(\mu,\nu)}(\iota)| \leq \frac{1}{2}|\epsilon_g^{(\mu,\nu)} + \epsilon_c^{(\mu,\nu)}|\omega^{(\mu,\nu)}(\iota)$ does not depend on specific m and n .
- If a cylindrical continuum branch, $\omega = \bar{v}_A/R_0|m\iota - n|$, $m = m_1, n = n_1$, crosses the line $\omega = \omega^{(\mu,\nu)}(\iota)$, it meets its “partner” with $m = m_1 \pm \mu, n = n_1 \pm \nu N$, and is split.
No branch of the Alfvén continuum dares to cross the gap!

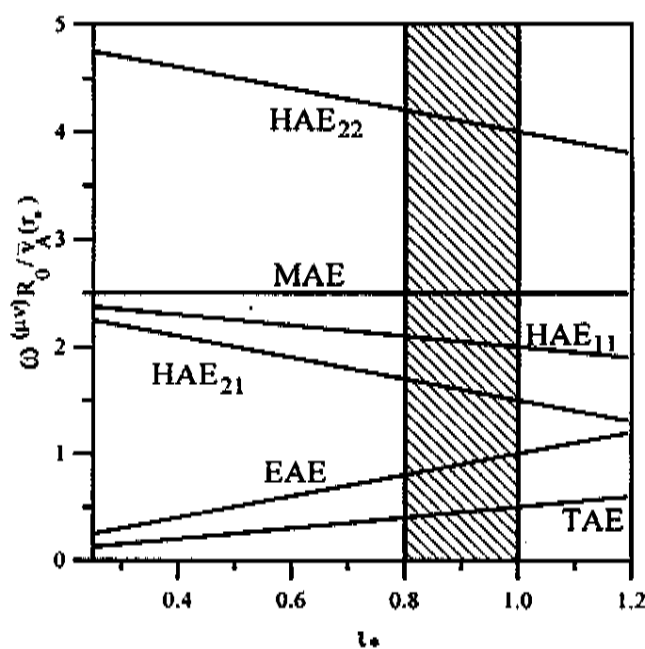
Continuum gaps in Helias

$$\omega_{m,n}(r_*) = \omega_{m+\mu, n+vN}(r_*) \Rightarrow \omega = \omega^{(\mu, v)} = \frac{Nv - \mu l_*}{2} \frac{V_A r}{2R_0}$$

$$l_* = \frac{2n + vN}{2m + \mu}$$

"*" refers to the point where the cylindrical continua intersect

Fig.1.
Alfvén continuum and high-frequency eigenmodes in optimized stellarators
Ya.L Kolesnichenko, V.V. Lutsenko, H. Wobig, Yu.V. Yakovenko, and O.P. Fesenyuk



- TAE - Toroidicity-induced Alfvén Eigenmodes ($\mu=1, v=0$)
- EAE - Ellipticity-induced Alfvén Eigenmodes ($\mu=2, v=0$)
- MAE - Mirror-induced Alfvén Eigenmodes ($\mu=0, v=1$)
- HAE _{μ, v} - Helicity-induced Alfvén Eigenmodes

Computation of the continuous spectrum

- Given \tilde{k} , the problem is decomposed to the set of Fourier harmonics $\tilde{k}_{\mu\nu} = \tilde{k} + \mu\iota - \nu N$. We do not demand that $\tilde{k} = m\iota - n$ for integer m and n (get rid of the periodicity condition).
- The matrices are truncated to finite ones by setting finite windows in m and n .

Problem which did not exist for tokamak spectra

Branches with arbitrarily large m and n can be found at any interval of $\tilde{k} = m\iota - n$. The branches that correspond to the margins of the windows are not approximated well and pollute the spectrum. The pollution is enhanced as the windows increase. Using a mesh for approximation does not solve the problem.

Remedy

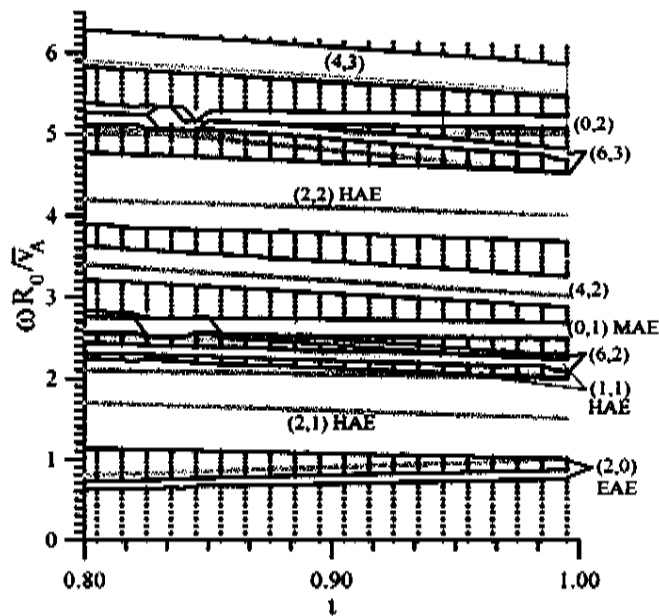
Filtering the eigenvectors. Several eigenvectors having the largest \tilde{k}_{00} component are selected.

The code **COBRA** (COntinuum BRanches of Alfvén waves) implementing this strategy has 3 modes of operation:

1. Scanning \tilde{k} at fixed ι , we find the continuum regions and gaps in the continuum.
2. Setting $\tilde{k} = (\mu\iota - \nu N)/2$ and selecting two eigenvectors, we find the “banks” of the (μ, ν) gap.
3. Setting $\tilde{k} = m\iota - n$ and selecting one eigenvector, we find the (m, n) branch.

Calculated gaps in the Alfvén continuum

Fig.4.
Alfvén continuum and high-frequency eigenmodes in optimized stellarators
Ya.I. Kolesnichenko, V.V. Lutsenko, H. Wobig, Yu.V. Yakovenko, and O.P. Fesenyuk



Lets, continuum

Black narrow lines, banks of the gaps

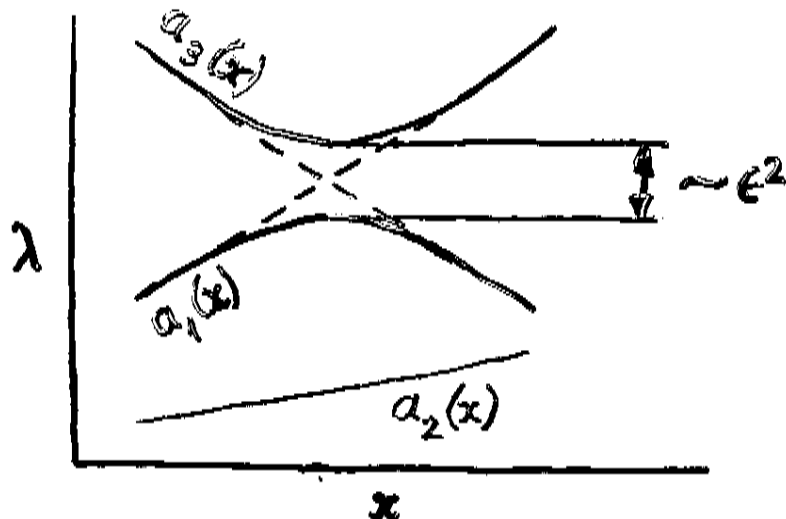
Thick grey lines, location of the gaps
at infinitely small ϵ_g, ϵ_c

Properties of the calculated continuum

- The gaps repel and compress each other, the ones located near the widest ($\mu = 2, \nu = 1$) gap being most strongly affected.
⇒ The 2-mode approximation fails for many of them.
- The “walls” between the gaps persist although some gaps would overlap if calculated in the 2-mode approximation.
- New (combination) gaps appear with (μ, ν) which correspond to no $g^{\psi\psi}$ or B harmonic, e.g., $(\mu, \nu) = (4, 2) = (2, 1) + (2, 1)$, $(0, 2) = (0, 1) + (0, 1)$, $(6, 3) = (2, 1) + (2, 1) + (2, 1)$, etc.

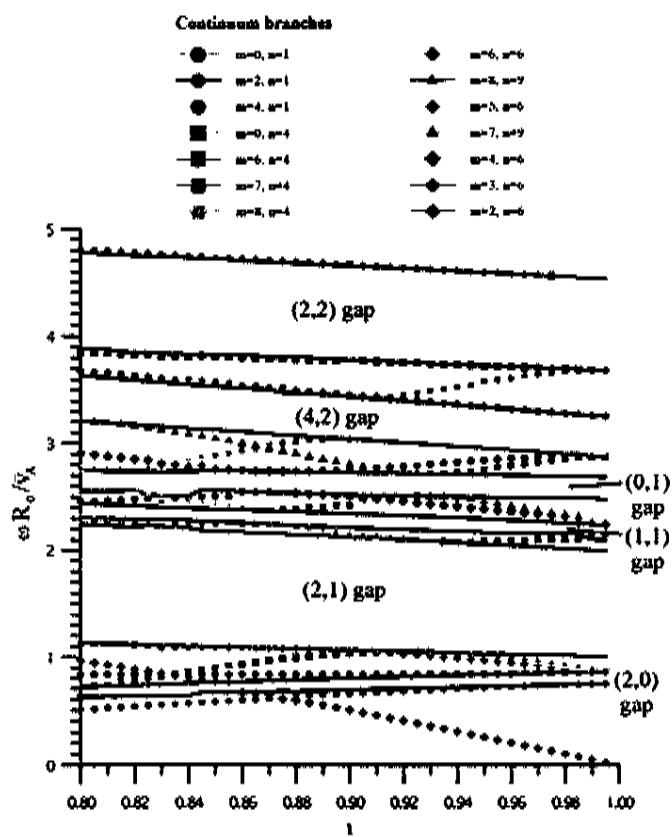
Mechanism of the formation of combination gaps

$$\begin{pmatrix} a_1(x) & \epsilon & 0 \\ \epsilon & a_2(x) & \epsilon \\ 0 & \epsilon & a_3(x) \end{pmatrix} \begin{pmatrix} \Phi_1 \\ \Phi_2 \\ \Phi_3 \end{pmatrix} = \lambda \begin{pmatrix} \Phi_1 \\ \Phi_2 \\ \Phi_3 \end{pmatrix}$$



The gap at the crossing of $a_1(x)$ and $a_3(x)$ is formed although there is no direct interaction between Φ_1 and Φ_3 components.

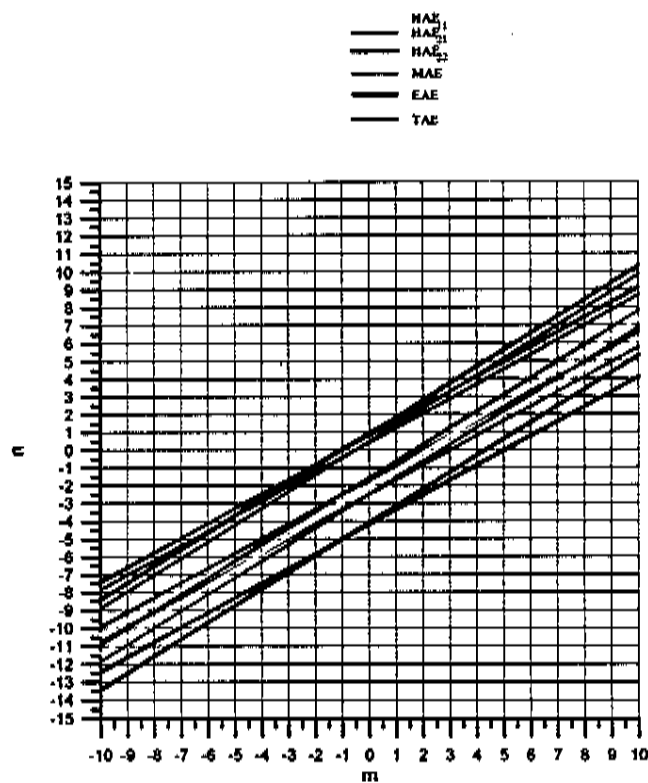
Fig.5.
Alfvén continuum and high-frequency eigenmodes in optimized stellarators
Ya.I. Kolesnichenko, V.V. Lutzenko, H. Wobig, Yu.V. Yakovenko, and O.P. Fesenyuk



"Corridors" of wavenumbers for which discrete AE may appear

$$\left\{ \begin{array}{l} |m\zeta_* - n| = |(m+\mu)\zeta_* - (n+\nu N)| = \frac{|\mu\zeta_* - \nu N|}{2} \\ l_{\min} \leq \zeta_* \leq l_{\max} \end{array} \right.$$

FIG.2.
Alfvén continuum and high-frequency eigenmodes in optimized stellarators
Ya.I. Kolesnichenko, V.V. Lubmenko, H. Wobig, Yu.V. Yakovenko, and O.P. Fesenyuk



HAE₂₁ equations

Expanding the AE equation into Fourier series, taking two equations for a pair of interacting modes and keeping terms of the order of ϵ only at the second radial derivatives, we obtain:

$$\begin{aligned} & \frac{\partial}{\partial r} r^3 \left(\frac{\omega^2}{\bar{v}_A^2} - k_{m,n}^2 \right) \frac{\partial E_{m,n}}{\partial r} + Q_{m,n} E_{m,n} \\ & + \frac{\partial}{\partial r} r^3 \left[\frac{\omega^2}{\bar{v}_A^2} \left(\frac{\epsilon_g^{(\mu\nu)}}{2} - 2\epsilon_B^{(\mu\nu)} \right) \right. \\ & \left. - k_{m,n} k_{m+\mu, n+\nu N} \frac{\epsilon_g^{(\mu\nu)}}{2} \right] \frac{\partial E_{m+\mu, n+\nu N}}{\partial r} = 0, \end{aligned}$$

$$\begin{aligned} & \frac{\partial}{\partial r} r^3 \left(\frac{\omega^2}{\bar{v}_A^2} - k_{m+\mu, n+\nu N}^2 \right) \frac{\partial E_{m+\mu, n+\nu N}}{\partial r} + Q_{m+\mu, n+\nu N} E_{m+\mu, n+\nu N} \\ & + \frac{\partial}{\partial r} r^3 \left[\frac{\omega^2}{\bar{v}_A^2} \left(\frac{\epsilon_g^{(\mu\nu)}}{2} - 2\epsilon_B^{(\mu\nu)} \right) - k_{m,n} k_{m+\mu, n+\nu N} \frac{\epsilon_g^{(\mu\nu)}}{2} \right] \frac{\partial E_{m,n}}{\partial r} = 0. \end{aligned}$$

where $\mu = 2$ and $\nu = 1$ determine the type of coupling,

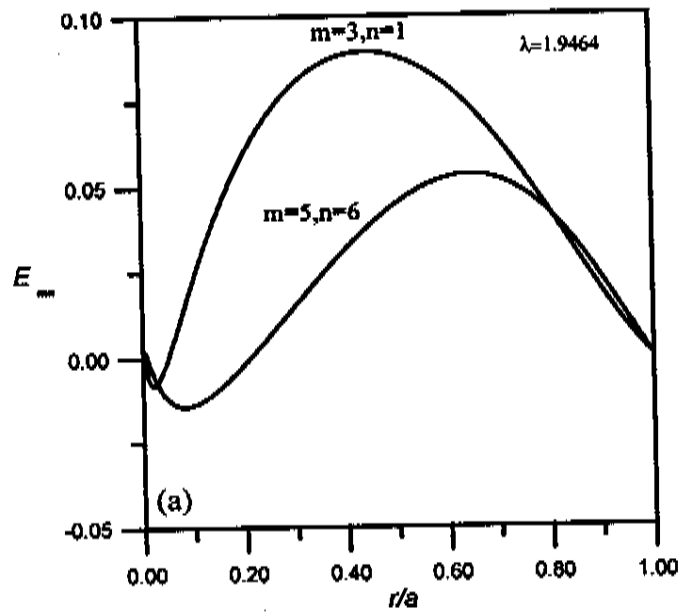
$$E = \Phi/r, k_{m,n} = (m\omega - n)/R_0,$$

$$Q_{m,n} = r \left(\frac{\omega^2}{\bar{v}_A^2} - k_{m,n}^2 \right) (1 - m^2) + r^2 \left(\frac{\omega^2}{\bar{v}_A^2} \right)'$$

The equations have been implemented in the code BOA (Branches Of Alfvén eigenmodes).

HAE₂₁

Upper part
of the gap



Lower part
of the gap

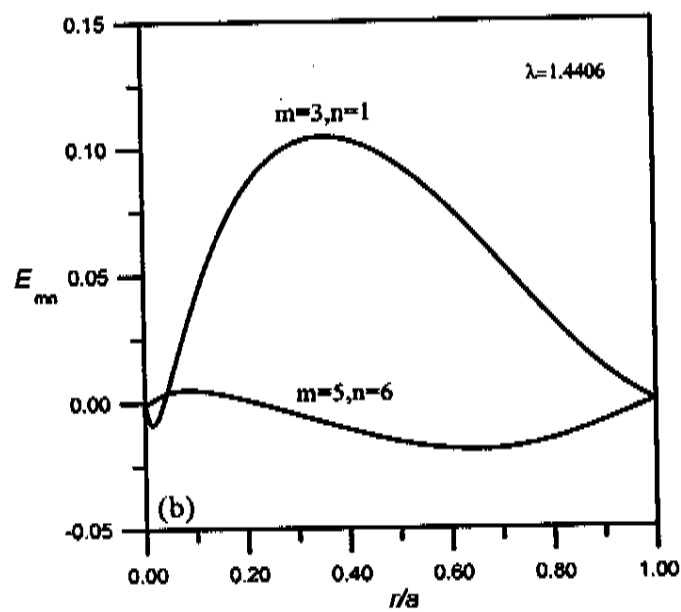


Fig. 6.
Alfvén continuum and high-frequency eigenmodes in optimized stabilators
Ya. I. Kolesnichenko, V.Y. Lutchenko, H. Wobig, Yu.V. Yakunin, and O.P. Pashen'yuk

Effect of the n inhomogeneity on the (2,1) gap.

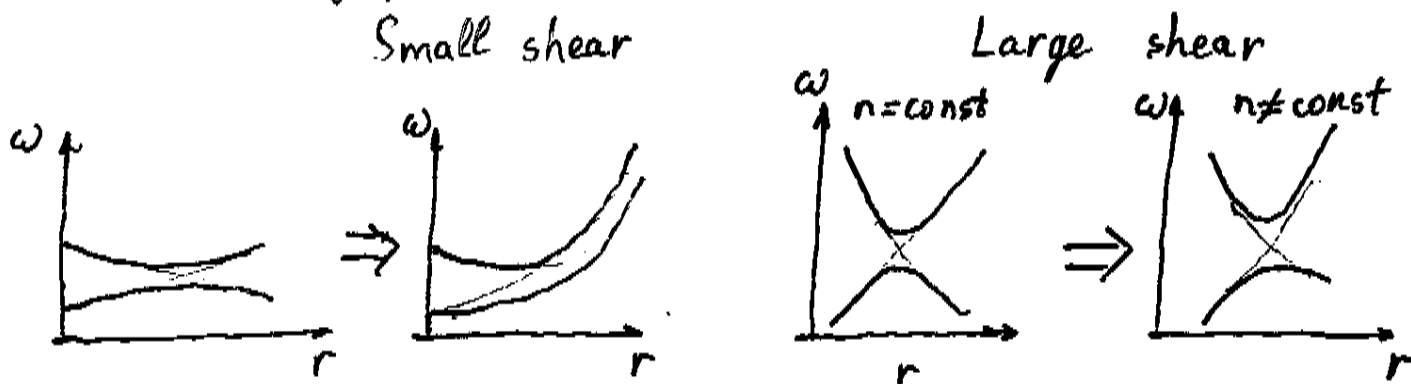
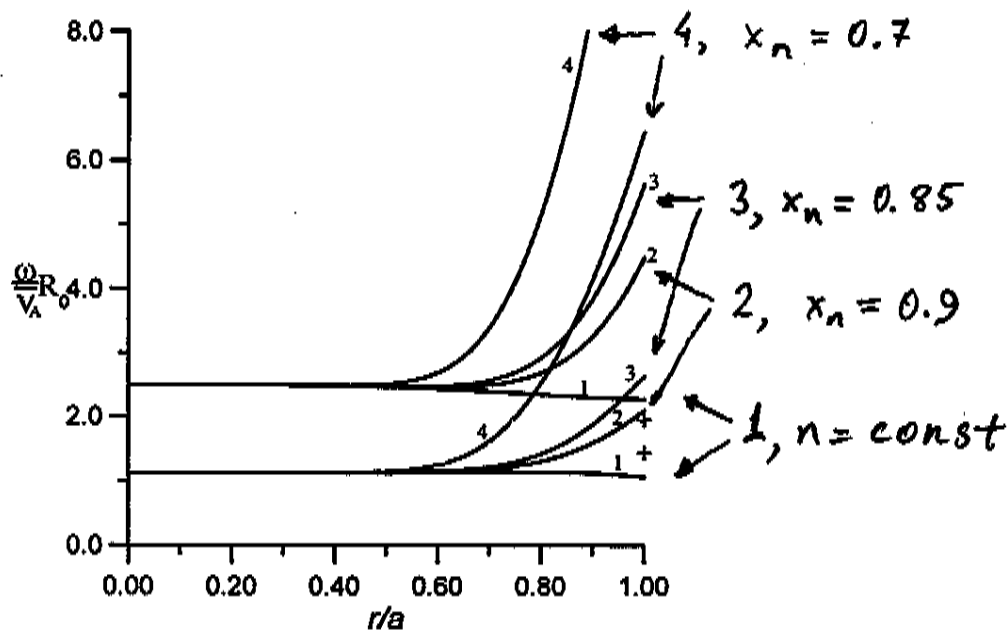


Fig.7.
Alfvén continuum and high-frequency eigenmodes in optimized stellarators
Ya.I. Kolesnichenko, V.V. Lutsenko, H. Wobig, Yu.V. Yakovenko, and O.P. Fesenyuk

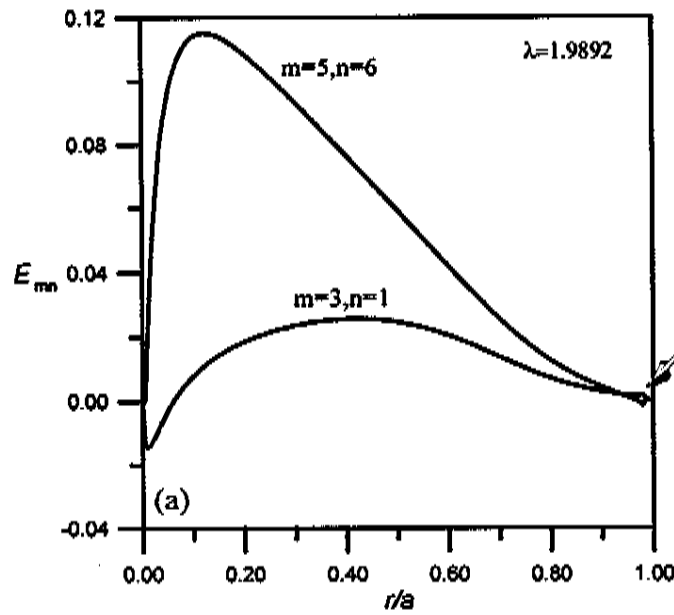


The gap for $(m,n) = (3,1)$ and $(5,6)$ modes

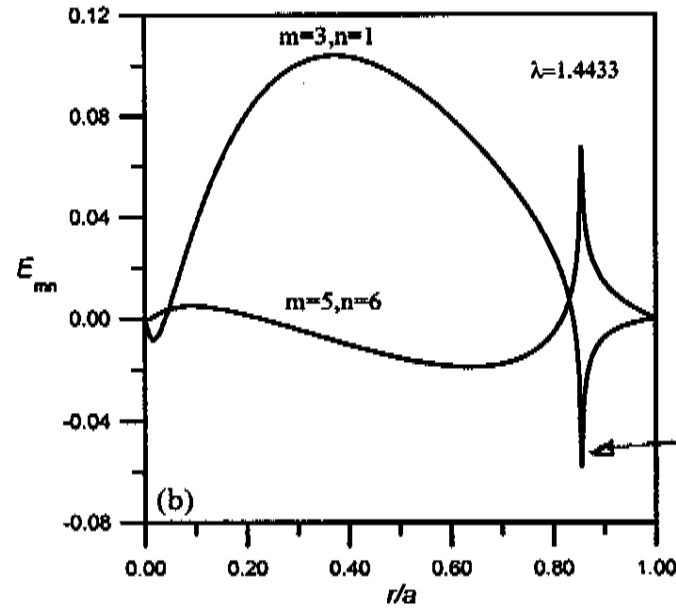
$$\rho(r) = \rho(0) [1 + r/(x_n a)]^{-1}$$

HAE_{21} , $n(r) \neq \text{const}$

Upper



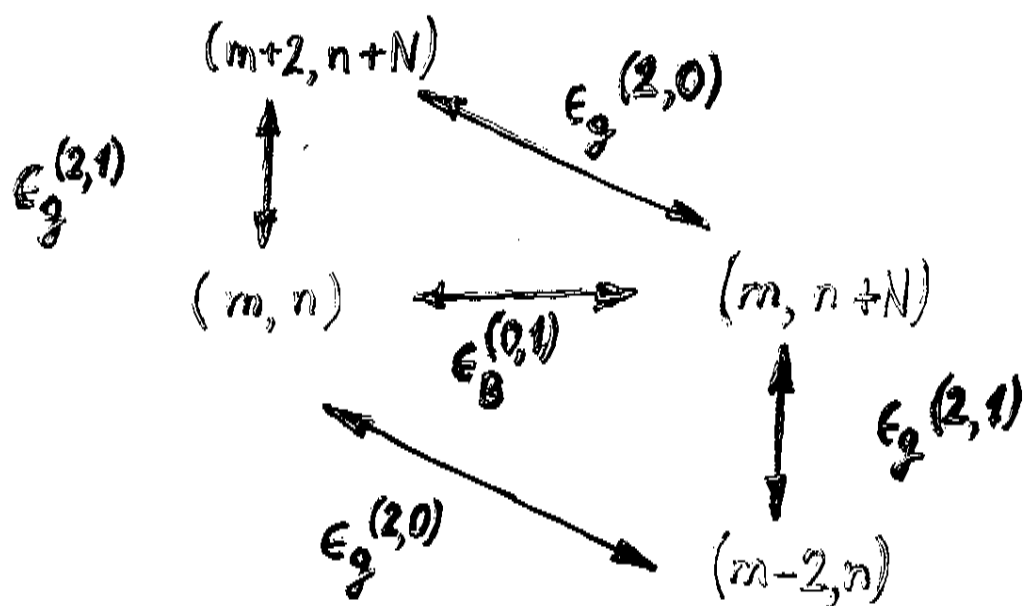
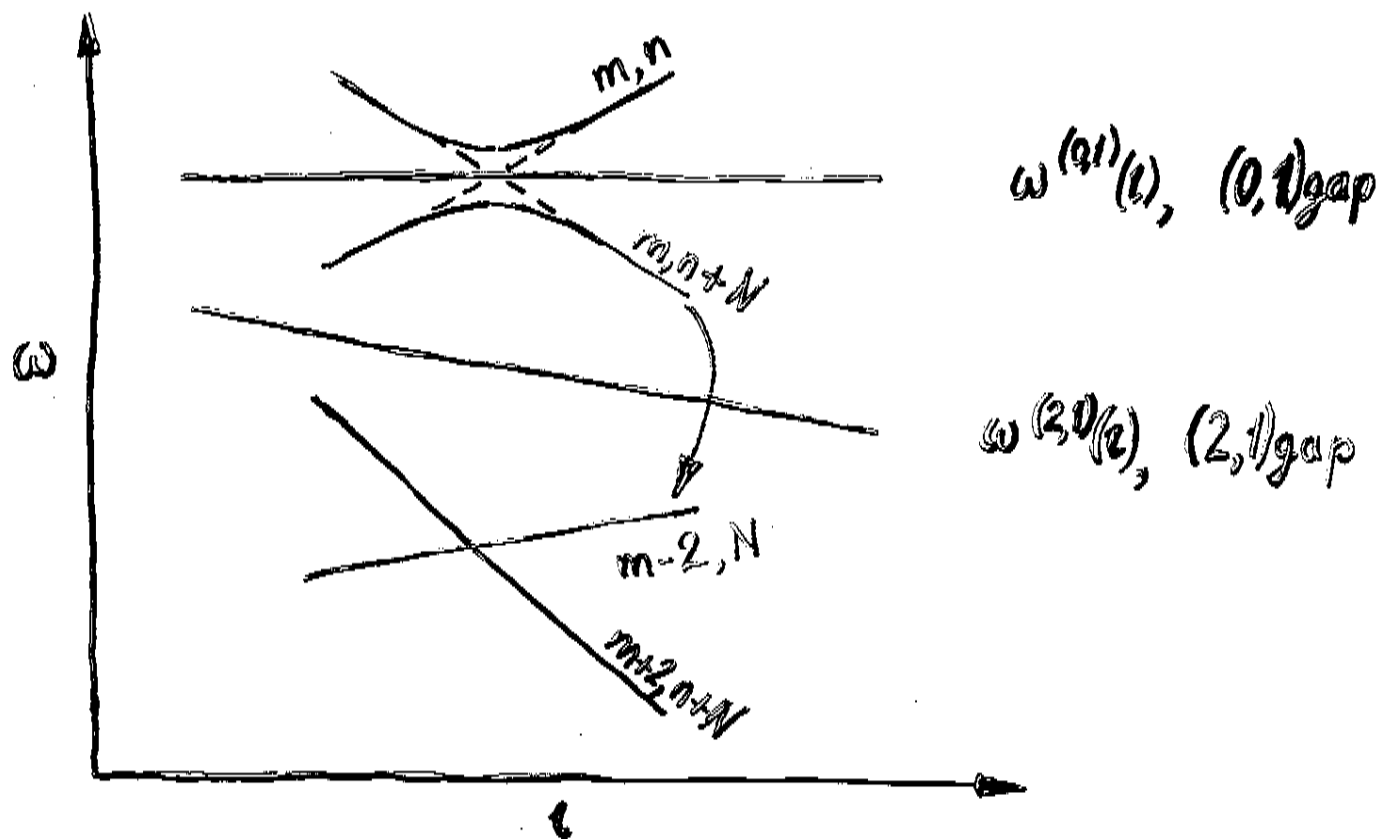
Lower



Crossing
with the
continuum

Fig. 9.
Alfvén continuum and high-frequency eigenmodes in optimized slabulations
Ya.I. Kondratenko, V.V. Lutsenko, H. Wobig, Yu.V. Yatsenko, and O.P. Fesenyuk

Effect of the (2,1) gap on the (0,1) gap.



MAE equations

We consider the interaction of the modes $(m+2, n+N) \iff (m, n) \iff (m, n+N) \iff (m-2, n)$

$$\begin{aligned}
& \frac{\partial}{\partial r} r^3 \left(\frac{\omega^2}{\bar{v}_A^2} - k_{m,n}^2 \right) \frac{\partial E_{m,n}}{\partial r} + Q_{m,n} E_{m,n} \\
& + \frac{\partial}{\partial r} r^3 \left[\frac{\omega^2}{\bar{v}_A^2} \left(\frac{\epsilon_g^{(01)}}{2} - 2\epsilon_B^{(01)} \right) - \frac{\epsilon_g^{(01)}}{2} k_{m,n} k_{m,n+N} \right] \frac{\partial E_{m,n+N}}{\partial r} \\
& + \frac{\partial}{\partial r} r^3 \left(\frac{\omega^2}{\bar{v}_A^2} - k_{m,n} k_{m+2,n+N} \right) \frac{\epsilon_g^{(21)}}{2} \frac{\partial E_{m+2,n+N}}{\partial r} \\
& + \frac{\partial}{\partial r} r^3 \left(\frac{\omega^2}{\bar{v}_A^2} - k_{m,n} k_{m-2,n} \right) \frac{\epsilon_g^{(20)}}{2} \frac{\partial E_{m-2,n}}{\partial r} = 0
\end{aligned}$$

$$\begin{aligned}
& \frac{\partial}{\partial r} r^3 \left(\frac{\omega^2}{\bar{v}_A^2} - k_{m,n+N}^2 \right) \frac{\partial E_{m,n+N}}{\partial r} + Q_{m,n+N} E_{m,n+N} \\
& + \frac{\partial}{\partial r} r^3 \left[\frac{\omega^2}{\bar{v}_A^2} \left(\frac{\epsilon_g^{(01)}}{2} - 2\epsilon_B^{(01)} \right) - \frac{\epsilon_g^{(01)}}{2} k_{m,n} k_{m,n+N} \right] \frac{\partial E_{m,n}}{\partial r} \\
& + \frac{\partial}{\partial r} r^3 \left(\frac{\omega^2}{\bar{v}_A^2} - k_{m,n+N} k_{m-2,n} \right) \frac{\epsilon_g^{(21)}}{2} \frac{\partial E_{m-2,n}}{\partial r} \\
& + \frac{\partial}{\partial r} r^3 \left(\frac{\omega^2}{\bar{v}_A^2} - k_{m,n+N} k_{m+2,n+N} \right) \frac{\epsilon_g^{(20)}}{2} \frac{\partial E_{m+2,n+N}}{\partial r} = 0
\end{aligned}$$

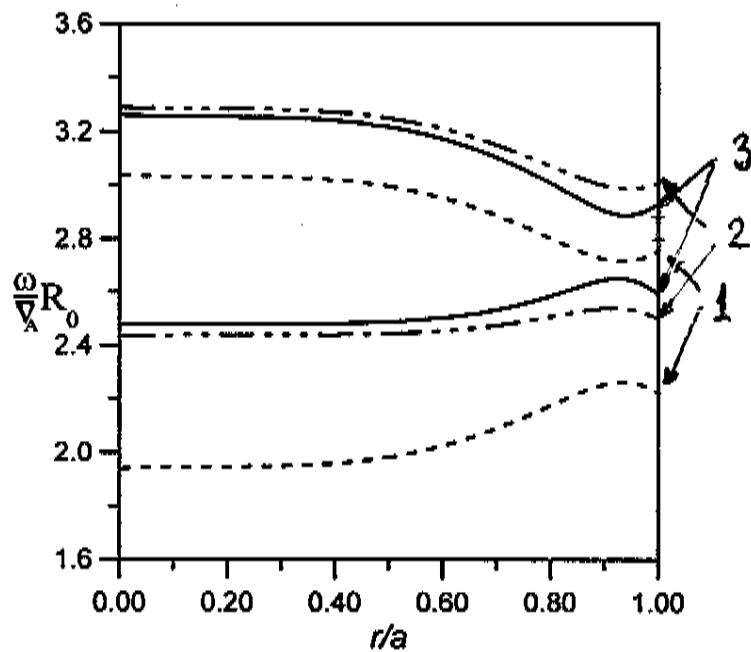
$$\begin{aligned}
& \frac{\partial}{\partial r} r^3 \left(\frac{\omega^2}{\bar{v}_A^2} - k_{m+2,n+N}^2 \right) \frac{\partial E_{m+2,n+N}}{\partial r} + Q_{m+2,n+N} E_{m+2,n+N} \\
& + \frac{\partial}{\partial r} r^3 \left(\frac{\omega^2}{\bar{v}_A^2} - k_{m,n} k_{m+2,n+N} \right) \frac{\epsilon_g^{(21)}}{2} \frac{\partial E_{m,n}}{\partial r} \\
& + \frac{\partial}{\partial r} r^3 \left(\frac{\omega^2}{\bar{v}_A^2} - k_{m+2,n+N} k_{m,n+N} \right) \frac{\epsilon_g^{(20)}}{2} \frac{\partial E_{m,n+N}}{\partial r} = 0
\end{aligned}$$

$$\begin{aligned}
& \frac{\partial}{\partial r} r^3 \left(\frac{\omega^2}{\bar{v}_A^2} - k_{m-2,n}^2 \right) \frac{\partial E_{m-2,n}}{\partial r} + Q_{m-2,n} E_{m-2,n} \\
& + \frac{\partial}{\partial r} r^3 \left(\frac{\omega^2}{\bar{v}_A^2} - k_{m,n+N} k_{m-2,n} \right) \frac{\epsilon_g^{(21)}}{2} \frac{\partial E_{m,n+N}}{\partial r} \\
& + \frac{\partial}{\partial r} r^3 \left(\frac{\omega^2}{\bar{v}_A^2} - k_{m-2,n} k_{m,n} \right) \frac{\epsilon_g^{(20)}}{2} \frac{\partial E_{m,n}}{\partial r} = 0
\end{aligned}$$

MAE gap

Fig.10.
Alfvén continuum and high-frequency eigenmodes in optimized stellarators
Ya.I. Kolesnichenko, V.V. Lutsenko, H. Wobig, Yu.V. Yakovenko, and O.P. Fesenyuk

$(m, n) = (4, 1)$ and $(4, 6)$



- 1, the MAE gap, two-mode approximation
- 2, 4 modes $\epsilon_g^{(21)} \neq 0$
- 3, 4 modes, $\epsilon_g^{(21)} \neq 0, \epsilon_g^{(20)} \neq 0$.

MAE, wave functions

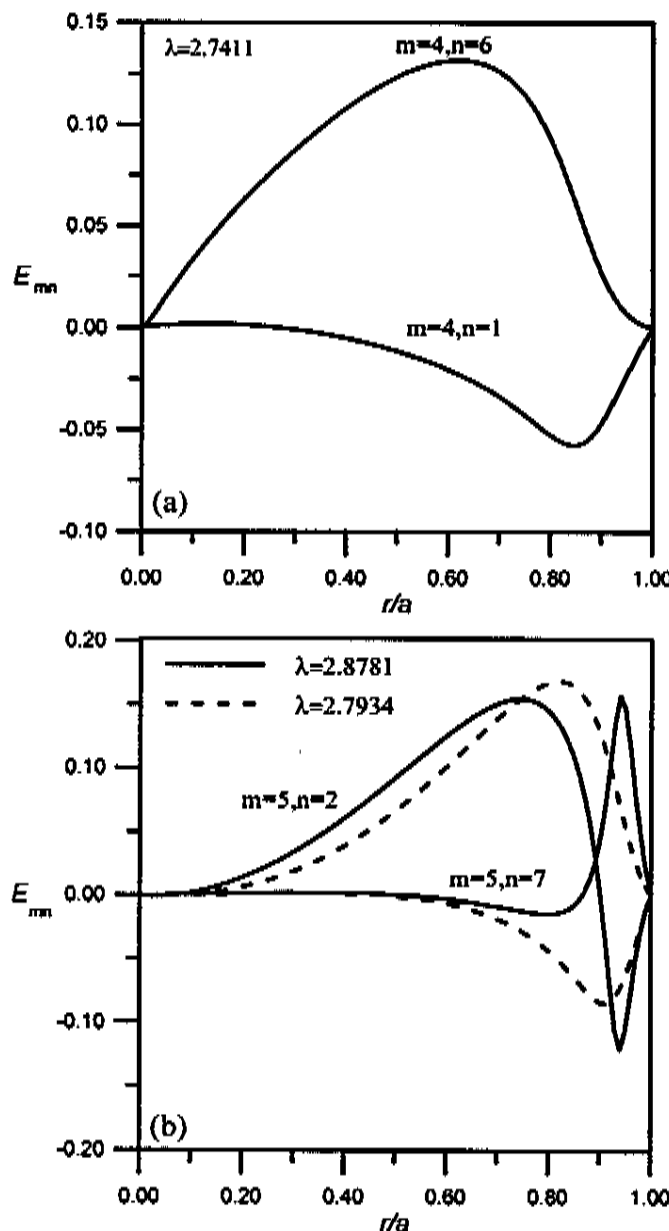


Fig. 11.
Alfvén continuum and high-frequency eigenmodes in optimized stellarators
Ya.I. Kolesnichenko, V.V. Lutsenko, H. Weigl, Yu.N. Yalovchenko, and O.P. Fedenyuk

Inhomogeneity of $n(\psi)$ kills discrete modes

Summary

- Equations of AE in a Helias have been derived.
- We has shown that the avoid-crossing phenomenon acts independently on the wavenumber, which results in “absolute” gaps in the Alfvén continuum.
- Two codes, COBRA for calculating the Alfvén continuum and BOA for caculating discrete AE, have been developed.
- The continuum gaps in the Helias have been calculated, the HAE_{21} , EAE, HAE_{22} , HAE_{42} and MAE gaps being the widest.
- We have shown that the elongation and rotation of the plasma cross section strongly affect the Alfvén spectrum in Helias. In general, gaps resulting from plasma shaping are more pronounced in Helias than those resulting from the B modulation.
- Secondary (combination) gaps have been found.
- Discrete HAE_{21} and MAE modes have been calculated.
- The density profile has been shown to be essential for existence and stability of non-localized discrete modes.